J. Membrane Biol. 150, 219–230 (1996)

The Journal of
Membrane
Biology

Large-conductance Calcium-activated Potassium Channels of Cultured Rat Melanotrophs

S.J. Kehl, K. Wong
Department of Physiology, University of British Columbia, Vancouver, B.C., V6T 1Z3, Canada

Received: 23 October/Revised: 15 December 1995

Abstract. A large conductance, Ca^{2+}-activated K^+ channel of the BK type was examined in cultured pituitary melanotrophs obtained from adult male rats. In cell-attached recordings the slope conductance for the BK channel was ≈190 pS and the probability (P_o) of finding the channel in the open state at the resting membrane potential was low (<<0.1). Channels in inside-out patches and in symmetrical 150 mM K^+ had a conductance of ≈260 pS. The lower conductance in the cell-attached recordings is provisionally attributed to an intracellular K^+ concentration of ≈113 mM. The permeability sequence, relative to K^+, was $K^+ > Rb^+$ (0.87) > NH_4^+ (0.17) > $Cs^+ \geqslant Na^+$ (≤0.02). The slope conductance for Rb^+ was much less than for K^+. Neither Na^+ nor Cs^+ carried measurable currents and 150 mM internal Cs^+ caused a flickery block of the channel. Internal tetraethylammonium ions (TEA^+) produced a fast block for which the dissociation constant at 0 mV (K_D(0 mV)) was 50 mM. The K_D(0 mV) for external TEA^+ was much lower, 0.25 mM, and the blocking reaction was slower as evidenced by flickery open channel currents. With both internal and external TEA^+ the blocking reaction was bimolecular and weakly voltage dependent. External charybdotoxin (40 nM) caused a large and reversible decrease of P_o. The P_o was increased by depolarization and/or by increasing the concentration of internal Ca^{2+}. In 0.1 μM Ca^{2+} the half-maximal P_o occurred at ≈100 mV; increasing Ca^{2+} to 1 μM shifted the voltage for the half-maximal P_o to −75 mV. The Ca^{2+} dependence of the gating was approximated by a fourth power relationship suggesting the presence of four Ca^{2+} binding sites on the BK channel.

Key words: Potassium channel — Permeability — Gating — Tetraethylammonium

Correspondence to: S.J. Kehl

Introduction

Most cells show an increase of K^+ permeability that can be activated by an increase of the cytoplasmic concentration of ionized or free calcium, Ca^{2+} (Latorre et al., 1989). This Ca^{2+}-activated K^+ permeability can be mediated by several types of ion channels that are categorized by their unitary conductances. In addition to a family of ''small'' conductance (<100 pS) Ca^{2+}-activated K^+ channels (SK) (Blatz & Magleby, 1986; Lang & Ritchie, 1987), there is a family of ''maxi'' or ''big'' conductance Ca^{2+}-activated K^+ channels (BK) that is characterized by a conductance of 200–300 pS in symmetrical 100–200 mM K^+ (Latorre et al., 1989). Studies of its ionic selectivity have shown that the BK channel is permeable to Rb^+ and NH_4^+ but is much less permeable, if at all, to Na^+ or Cs^+ ions. Organic compounds that block BK channels include tetraethylammonium ions (TEA^+) (Blatz & Magleby, 1984; Yellen, 1984*a*; Wong & Adler, 1986) and charybdotoxin (Anderson et al., 1988).

Unlike some of the SK channels, the gating of the BK channel is also influenced by the membrane potential. Thus, with a fixed concentration of Ca^{2+} at its cytoplasmic face, the probability (P_o) of finding the BK channel in the open state can be increased by membrane depolarization. On the other hand, at a fixed membrane potential the P_o can be increased by an increase of Ca^{2+}. The Ca^{2+} sensitivity of BK channels does, however, vary markedly between different cell types (Barrett, Magleby & Pallotta, 1982; Maruyama et al., 1983).

Melanotrophs of the pars intermedia of the rat pituitary gland exhibit electrical activity that reflects, at least in part, the interactions between voltage-dependent Na^+, Ca^{2+} and K^+ channels (Cota, 1986; McBurney & Kehl, 1988). In this paper, we characterize a BK-type channel found in the rat melanotroph in terms of: (i) its ionic selectivity; (ii) the blocking effects of charybdotoxin as well as internal and external TEA^+, and (iii) the voltage- and Ca^{2+}-dependence of gating. This undertaking is the

first step towards determining the contribution of BK channels to the electrical activity of melanotrophs.

A preliminary account of these findings has been communicated to the Society for Neuroscience (Kehl et al., 1995).

Materials and Methods

Cell Culture

The animals used in this study were treated in accordance with the principles and guidelines of the Canadian Council on Animal Care. Adult male rats (Wistar, 200–300 g) were exposed to CO_2 gas to produce unconsciousness prior to decapitation. Melanotrophs were obtained from excised pituitary glands by using techniques described previously (Kehl, Hughes & McBurney, 1987). Following enzymatic treatment and mechanical dispersion of neurointermediate lobe tissue, cells were placed onto collagen-coated (Sigma, Type VII, from rat tail) Aclar (Proplastics, Linden, NJ) coverslips. The feed medium, which was changed every 3–4 days, consisted of equal portions of bicarbonate-buffered Ham's F-12 medium and Dulbecco's modified Eagle medium. The feed medium was supplemented with fetal bovine serum (10% V/V), 15 mM N-2-hydroxyethylpiperazine-N′-2-ethanesulphonic acid (HEPES), 2 mM glutamine, 5 μg/ml insulin, 5 μg/ml transferrin and 5 ng/ml of sodium selenite. Penicillin (100 units/ml) and streptomycin (100 units/ml) were components of the feed medium only during the first 5–7 days *in vitro*; 1 μM cytosine arabinoside was included after 5–7 days *in vitro* to inhibit mitotic division of background cells. Recordings were made from cells maintained *in vitro* for 1 day to 3 weeks.

Single Channel Recording

BK channels were recorded at room temperature (≈22°C) from phase-bright spherical cells of the type that have been shown previously to fire action potentials and have voltage-gated Na^+, Ca^{2+} and K^+ currents (*see* Fig. 1 of McBurney & Kehl, 1988) and which stain intensely for α-MSH (*not shown*). Patch electrodes were pulled from 1.5 mm outside-diameter borosilicate glass tubing (Corning # 7052, A-M Systems, Everett, WA) and coated near the tip with Sylgard 184 elastomer (Dow Corning, Midland, MI) prior to fire-polishing. Pipette resistances were typically between 5 and 10 MΩ. Current and voltage signals, referenced to a 150 mM NaCl-containing agar bridge, were recorded with a List-Electronic EPC-7 (Darmstadt, Germany) patch clamp amplifier.

Electrode offsets were nulled prior to the formation of a tight seal (greater than 1 GΩ). Currents were referenced to the extracellular face of the membrane regardless of the recording configuration. Positive charge flowing from the cytoplasmic face to the extracellular face of the channel represents a positive current and is shown as an upward deflection from the channel-closed current level. In the current traces, where necessary, the closed state of the channel is indicated by the letter C and the open state by the letter O with a subscript to denote the number of channels open. Voltages have not been compensated for liquid junction potentials.

Signals stored on magnetic tape (d.c. — 10 kHz) were low-pass filtered at 2–3 kHz (−3 dB, 4-pole Bessel) and digitized at a sampling frequency of 5–10 kHz by a 12-bit LabMaster A-to-D interface (Scientific Solutions, Solon, OH) controlled by pCLAMP software (Axon Instruments, Foster City, CA). Digitized data were analyzed on a 80486-based computer using routines in pCLAMP. Mean single channel currents were measured from an all-points histogram or from an events lists constructed from 5–120 sec segments of channel activity. With the all-points histogram the unitary current was taken as the difference between the means of the Gaussian curves fitted to the binned data using the Levenberg-Marquardt least squares fitting method. For the generation of an events list the threshold for event detection was set at 50% of the mean single channel current and a dead time of 90 μsec was used.

Measurements of ion selectivity were done with inside-out patches in bi-ionic conditions. The patch pipette (external) solution contained 150 mM KCl (Table) and the internal solution contained, in the form of the chloride salt, 150 mM of NH_4^+ or alkali metal ions. Ionic activities (a), derived from activity coefficients interpolated from tabulated values (Robinson & Stokes, 1965), were (in mM): 111, 113, 110, 111 and 108 for K^+, Na^+, Rb^+, NH_4^+ and Cs^+, respectively. To obtain values for absolute permeabilities, *I/V* relationships were fitted to the Goldman-Hodgkin-Katz (GHK) constant field equation,

$$I = \left(\frac{VF^2}{RT}\right)\left(\frac{P_X a_{X,i} - P_K a_{K,o}\exp\left(-\frac{VF}{RT}\right)}{1-\exp\left(-\frac{VF}{RT}\right)}\right) \quad (1)$$

where V is the membrane voltage, P_X and P_K are the permeabilities (cm^3/sec) for the test cation and external K^+, and $a_{X,i}$ and $a_{K,o}$ represent the activities of the test cation and external K^+, respectively. F, R, and T have their usual meanings; a value of 25.43 mV was used for RT/F. Some of the assumptions on which the derivation of the GHK equation is based, e.g., that ion fluxes are independent, are probably not valid for most BK channels. However, as noted by Hille (1992), the GHK equation has the important advantage that it summarizes measurements in terms of a single parameter, absolute permeability or permeability ratios. And, with a few exceptions, reasonably close fits of the data to the GHK equation were obtained. Since our primary aim was to characterize the selectivity of the BK channel, rather than model the permeation pathway, we chose not to use an approach based on rate theory (Yellen, 1984*a*).

Channel open probability (P_o) was calculated from the equation,

$$P_o = (T_1 + T_2 \ldots + T_N)/NT_{\text{total}} \quad (2)$$

where T_1, T_2 . . . and T_N represent the sum of the time intervals when at least *1, 2* . . . or N channels are open, T_{total} is the duration of the data segment (typically 10 sec) and N is the number of active channels in the patch. N was estimated under conditions that maximized P_o, i.e., 10 μM Ca^{2+} and strong depolarization (50–80 mV). In outside-out patches where the number of active channels could not be counted the value NP_o was calculated as,

$$NP_o = (T_1 + T_2 \ldots + T_N)/T_{\text{total}} \quad (3)$$

A nonlinear, least-squares fitting routine (SYSTAT, Evanston, IL) was used to fit the data to model equations. The goodness of the fit is indicated by the coefficient of determination (r^2). Comparison of means was done by using the Tukey HSD method. A P value less than 0.05 was considered to be significant.

Solutions

The compositions of bath and pipette solutions are indicated in the Table. Bath solution represents the medium perifusing the cell for cell-attached recordings, the internal solution for inside-out recordings and the external solution for outside-out recordings. Pipette solution represents the external solution for cell-attached or inside-out patches but is the internal solution for outside-out patches. Ionized

Table. Composition of solutions (in mM except where noted)

Solution	NaCl	KCl	XCl	NMDG	$MgCl_2$	$CaCl_2$[a]	EGTA	Glucose	TEA
Bath									
Control	128	3.5			1	10		5	
140 NaCl	140	3.5			3			5	
150 XCl			140	≈8	1	0.9–0.95 (0.5–1 μM)	1		
0.1 μM Ca^{2+}		150			1	.644	1		
0.5 μM Ca^{2+}		150			1	.9	1		
1.0 μM Ca^{2+}		150			1	.95	1		
10 μM Ca^{2+}		150			1	1.01	1		
TEA_i		110		0–40	1	0.9 (.5 μM)	1		0–40
TEA_o	140	3.5			3				0–0.8
Pipette									
150 KCl		150			1	.975 (2 μM)	10		
150 NaCl	150				1	.975 (2 μM)	10		

[a] Total and (ionized) calcium; Most solutions were buffered to pH 7.4 with 10 mM HEPES and either NaOH (control, 140 NaCl, TEA_o, NaCl) or KOH (0.1–10 μM Ca^{2+}, TEA_i, 150 KCl). For the 150 XCl solutions, where X represents an alkali metal ion or NH_4^+, the pH was adjusted to 7.4 with 10 mM HEPES and N-methyl-D-glucamine (NMDG) so that there was no significant content of other alkali metal ions.

Ca^{2+} concentrations were obtained by using the appropriate Ca^{2+}-EGTA (ethyleneglycol-bis(β-aminoethylether)-N,N,N′,N′-tetraacetic acid) buffers computed by using Max Chelator software (Stanford University, CA) employing the stability constants of Martell & Smith (1974). Application of drugs or test solutions to cell-attached, inside-out or outside-out patches was done by bath perfusion. The small volume of the bath (<400 μl) and a high flow rate (1–2 ml/min) allowed complete exchange of the bath solution in less than 1 min. Solution flow was stopped during recordings.

Compounds were obtained from Sigma Chemical (St. Louis, MO) except for charybdotoxin which was purchased from Peninsula Laboratories (Belmont, CA).

Results

Conduction Properties of the BK Channel

Typical current/voltage (*I/V*) relationships for BK channels when the pipette contained 150 KCl solution (Table) and the cell was bathed in control medium (Table) are shown in Fig. 1. For a potassium-selective channel the unitary current (I) is equal to the product of the chord conductance (γ) and the driving force for ion movement ($V-E_K$) where V is the voltage across the patch and E_K is the potassium equilibrium potential calculated from the Nernst equation. Since in the cell-attached mode the value for V depends on the difference between the resting membrane potential ($V_{resting}$) and the applied pipette voltage ($V_{pipette}$) the modified ohmic equation can be rewritten,

$$I = \gamma(V_{resting} - V_{pipette} - E_K) \quad (4)$$

If a_K is the same on both sides of the membrane then E_K is equal to zero and the zero current level will occur when $V_{resting} = V_{pipette}$. This means that in Fig. 1 where I is plotted against $V_{resting} - V_{pipette}$, the resting membrane potential ranges between cells from −30 to −55 mV in agreement with the results of whole-cell recordings (McBurney & Kehl, 1988).

To reduce the uncertainty arising because $V_{resting}$ is unknown, the conventional approach is to depolarize the attached cell by bathing it in a high K^+ solution. Graphed in Fig. 2*B* are the results obtained from seven different patches where the bathing solution was the same as the pipette solution (150 KCl in the Table). As expected for a decrease of $V_{resting}$ under these conditions, the *x*-intercept, relative to the data of Fig. 1, was shifted to the left.

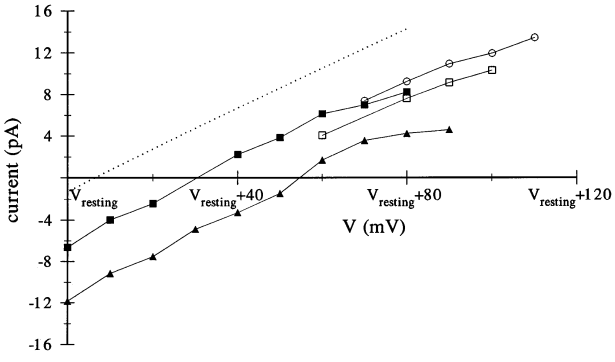

Fig. 1. The *I/V* relationship for the BK channel in the cell-attached configuration. The voltage across the patch (V) in this mode is equal to the unknown resting potential ($V_{resting}$) minus the pipette voltage ($V_{pipette}$). At the zero current level $V_{resting} = V_{pipette}$ assuming the concentration of the permeant ion is symmetrical. In two cells, (○, □) there was no measurable channel activity for $V_{pipette} > -60$ mV. Two other cells (■, ▲) were atypical in that channel opening occurred at $V_{resting}$. For comparison with responses in which the attached cell was depolarized the best fit to the data of Fig. 2 has been redrawn here as a broken line.

Illustrated in Fig. 2*A* are representative currents, recorded at a pipette potential of −60 mV from the same patch first in the depolarized cell-attached mode and subsequently in the inside-out configuration. The stippled lines superimposed on the traces from the inside-out recordings mark the current level of the open channel(s) in the cell-attached mode and underscore the larger current amplitude in the excised patch in symmetrical 150 mM K^+. The slope conductance for depolarized cell-attached recordings is ≈190 pS (Fig. 2*B*) whereas with inside-out patches in symmetrical 150 mM K^+ it is ≈260 pS (Fig. 3*B*).

A similar disparity between the single channel conductance in cell-attached and excised patches has been observed in smooth muscle BK channels and, since channel conductance is concentration-dependent (*see* Eq. 5), the difference was attributed to the fact that a_K was lower in the cytoplasm (Muraki, Imaizumi & Watanabe, 1992). Muraki and his colleagues estimated a value of 104 mM

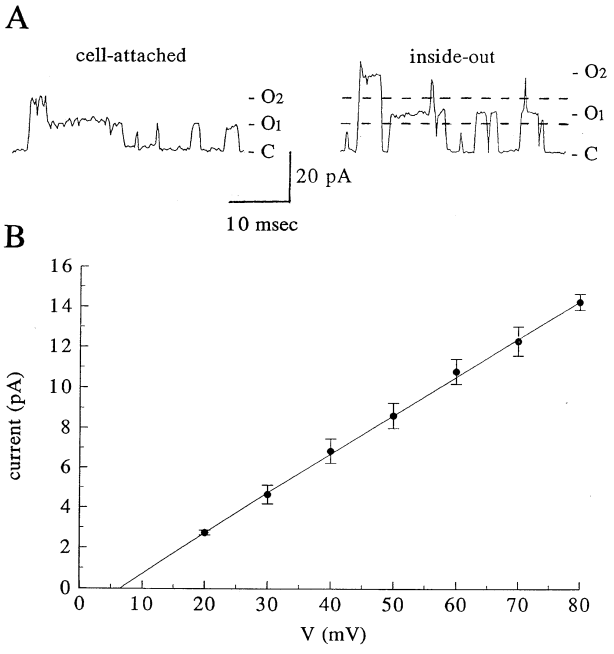

Fig. 2. Open channel currents in the cell-attached mode when the cell was depolarized by 150 mM K_o^+. (*A*) Current traces recorded from the same patch of membrane in the cell-attached and then in the inside-out configuration. Note the increase of the single channel current after forming the inside-out patch. Assuming the membrane potential in the cell-attached recording is 0 mV then the potential across the patch is 60 mV in either recording. The patch pipette solution and the internal solution (inside-out only) contained 150 mM K^+. In this and subsequent traces, currents above the closed level (C) represent cation movement from the cytoplasmic to the extracellular face of the channel and are positive. The stippled lines in the right-hand trace represent the open channel current levels of the cell-attached recording. (*B*) The *I/V* relationship derived from 7 patches on depolarized cells. Using a value of 111 mM for $a_{K,o}$, the best fit ($r^2 = 0.99$) was obtained with $P_K = 5.5 \times 10^{-13}$ cm^3/sec and $a_{K,i} = 86$ mM. The slope of the line is ≈190 pS.

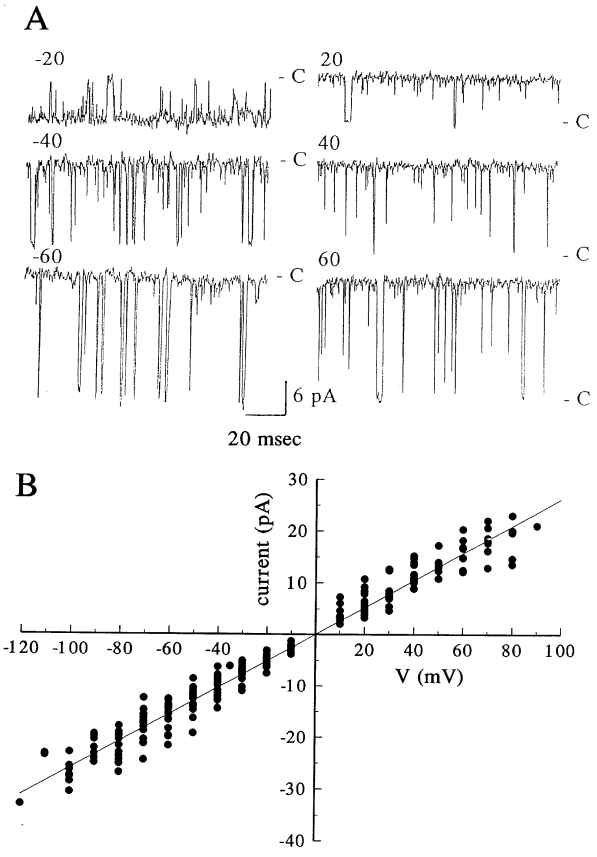

Fig. 3. Unitary BK channel currents recorded from inside-out patches. (*A*) Numbers above each trace represent the potential across the patch. Note that aside from affecting the amplitude and direction of the current, depolarization increased the probability of finding the channel in the open state (*cf.* Fig. 10). (*B*) A slope of 261 pS (95% C.L. 256–267) was fitted to the *I/V* relationship derived from 9 inside-out patches in symmetrical 150 mM K^+. As has been reported for other BK channels there was a large variability of the unitary currents at a given voltage.

for $[K^+]_i$ by fitting their cell-attached *I/V* data to the GHK equation (Eq. 1). Using the same approach, the best fit ($r^2 = 0.99$) of the data of Fig. 2*B* gave an $a_{K,i}$ of 86 mM which, assuming an activity coefficient similar to that in aqueous solutions, corresponds to a $[K^+]_i$ of 113 mM. The analysis was simplified by setting $V_{resting}$ to 0 mV, an assumption that has not been directly validated. The best fit to the GHK equation (solid line of Fig. 2*B*) also gave an zero current voltage of 6.5 mV and a value of 5.5×10^{-13} cm^3/sec for the absolute K^+ permeability. To show that the slope conductance was similar when the attached cell had not been depolarized by high K^+ the best-fit line of Fig. 2*B* is shown in Fig. 1 as a broken line.

The P_o in cell-attached recordings was not analyzed since *N* could not be determined. In greater than 95% of the cells studied in control medium (Table) there was no BK channel activity at $V_{resting}$. Depolarization of the membrane patch could increase the frequency and duration of channel openings but even at $V_{resting}$ + 100 mV

NP_o was typically low (<0.5). Two notable exceptions are evident in Fig. 1 where BK channel openings were observed in cells with normal resting potentials of approximately −30 (■) and −55 mV (▲).

Subsequent experiments analyzing the selectivity of the conduction pathway of the BK channel were done with inside-out patches. Except for the experiments of Fig. 4*A* (○), the pipette solution always contained 150 mM KCl (Table) and for control responses the bath solution contained 150 mM KCl (Table) to allow the unequivocal identification of the BK channel by its large conductance. Bath-applied test solutions contained 150 mM of K^+, Na^+, Rb^+, NH_4^+ or Cs^+ and 0.5–1 μM Ca^{2+}.

Analyses of membrane currents in inside-out patches are simplified by the fact that $V_{resting}$ is zero and the activities of ions at both faces of the channel are known. We first examined the *I/V* relationship for the BK when K^+ was the only permeant ion and its concentration was the same on each side, i.e., the concentration was symmetrical. Under these conditions Eq. 1 simplifies to,

$$I = \frac{P_K F^2 a_K}{RT} V \qquad (5)$$

which is equivalent to the modified ohmic equation, $I = \gamma(V - E_K) = \gamma V$ (since E_K is zero) and, as noted above, indicates that the single channel conductance is proportional to a_K. The current traces of Fig. 3*A* show, as expected, that the amplitude and direction of the current was proportional to the membrane voltage. As with BK channels in other cell types (Yellen, 1984*a*; Lang & Ritchie, 1987) there was some variability of the single channel conductance (Fig. 3*B*). A P_K of 6.2×10^{-13} cm^3/sec (95% confidence limits (C.L.) 6.1–6.3 × 10^{-13} cm^3/sec) was obtained from a fit of the data to the GHK equation. When fitted to the modified ohmic equation a value of 261 pS (95% C.L. 256–267 pS) was obtained for the conductance, γ.

Replacing external K^+ with Na^+ to mimic physiological ionic gradients produced a nonlinear *I/V* relationship where only outward currents, carried by K^+, were seen and the extrapolated reversal potential was −80 mV (Fig. 4*A*(○)). Values of 0.098×10^{-13} cm^3/sec (95% C.L. −0.28−0.48 × 10^{-13} cm^3/sec) and 6.3×10^{-13} cm^3/sec (95% C.L. 6.1–6.5 × 10^{-13} cm^3/sec) were obtained for P_{Na} and P_K, respectively, giving a permeability ratio, P_{Na}/P_K, of less than 0.02. With the opposite arrangement of solutions, e.g., 150 mM Na^+_i and 150 mM K^+_o, only inward K^+ currents were seen (Fig. 4*B*) and the extrapolated reversal potential was 76 mV (Fig. 4*A*(●)). Although P_K decreased to 4.9×10^{-13} cm^3/sec (95% C.L. 4.8–5.0 × 10^{-13} cm^3/sec), the value for P_{Na} was unchanged and the channel retained its high selectivity for K^+ over Na^+ ($P_{Na}/P_K = 0.02$).

Currents at 40 mV (center trace of Fig. 5*A*) show the

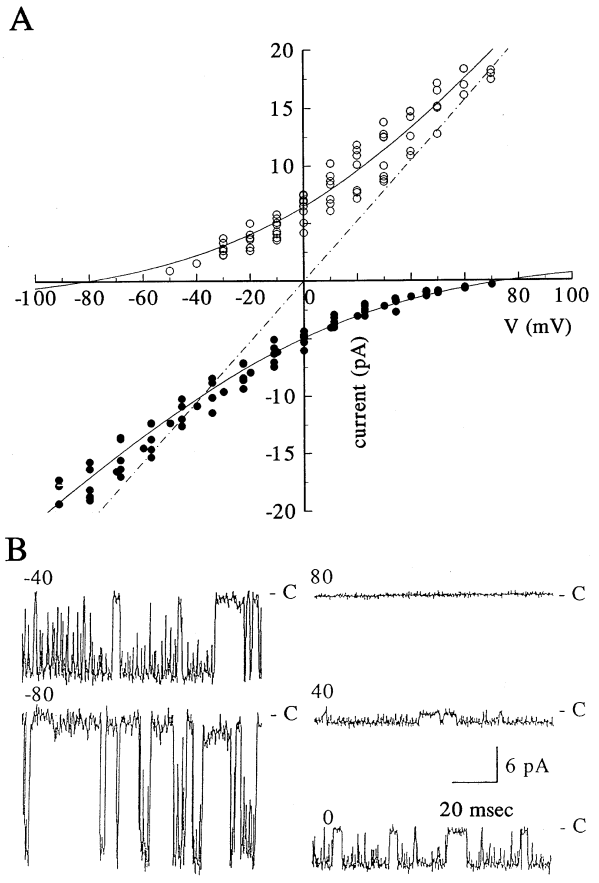

Fig. 4. (*A*) An asymmetrical distribution of K^+ produces a nonlinear *I/V* relationship. Currents evoked in 150 mM K^+_i and 150 mM Na^+_o (○) or 150 mM Na^+_i and 150 mM K^+_o (●) are plotted. Unbroken lines represent the fits of the two data sets to the GHK equation (Eq. 1, *see* text for details). For comparison, the best fit of the *I/V* relationship that was obtained in symmetrical 150 mM K^+ (*cf.* Fig. 3*B*) is redrawn here (stippled line). The traces in *B* show typical currents recorded with 150 mM K^+_o and 150 mM Na^+_i.

effect of switching over to (downward arrow) and back from (upward arrow) a bath (internal) solution in which 150 mM Rb^+ replaced 150 mM K^+. The upper and lower traces of Fig. 5*A* show selected portions of the center trace at expanded time bases. The graded decline and recovery of the single channel current signifies that the small outward Rb^+ currents reflect ion movement through BK channels rather than some other channel type. In the Rb^+ solution the single channel current is 1.5 pA (*d* in Fig. 5*A*) as compared to 10.3 pA in the control (*a* in Fig. 5*A*) and recovery responses.

Plotted in Fig. 5*B* is the *I/V* relationship obtained from 4 patches with 150 mM K^+_o and 150 mM Rb^+_i. Because a poor fit (broken line of Fig. 5*B*) to the GHK equation was obtained when both inward and outward current responses were used, the fitting routine was constrained to include only the data associated with inward currents. This approach (unbroken line of Fig. 5*B*) gave

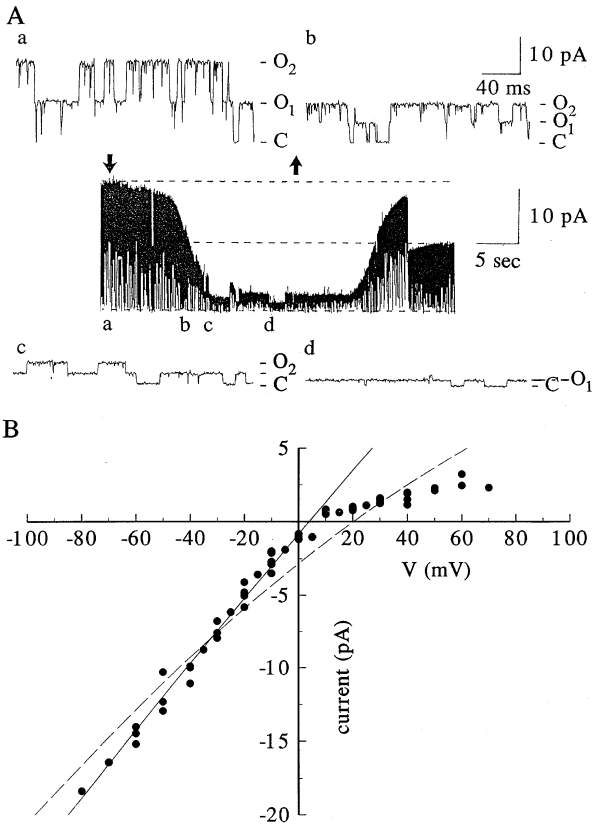

Fig. 5. Rb^+ ions permeate the BK channel almost as well as K^+ but the channel conductance is much lower with Rb^+ as the charge carrier. (*A*) The center trace shows the change of the BK channel current in an inside-out patch, at 40 mV, after switching over to (↓) and back from (↑) a bath solution in which 150 mM Rb^+ was completely substituted for 150 mM K^+. The control and recovery currents carried by K^+ were approximately sevenfold greater than with Rb^+ as the charge carrier. Currents at the times indicated by the letters below the center trace are shown at a much higher time resolution in traces a–d. (*B*) The P_{Rb} was slightly less than P_K as shown by a reversal potential near 0 mV in bi-ionic conditions. A better estimate of the reversal potential was obtained when the inward currents (unbroken line) rather than the entire range of data (stippled line) were fitted to the GHK equation.

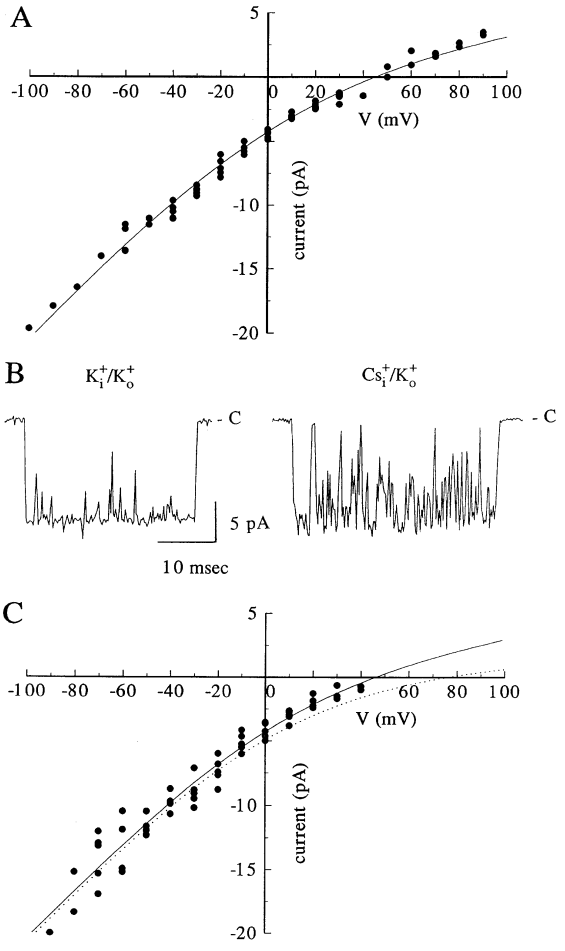

Fig. 6. The fit of the GHK equation to the *I/V* data with NH_4^+ as the major internal cation gave an estimate of 45 mV for the reversal potential and a P_{NH4}/P_K of 0.17. (*B*) After switching from an internal (bath) solution containing 150 mM K^+ (symmetrical K^+) to one containing 150 mM Cs^+ there was flickering of the channel current. In (*C*), current amplitudes with 150 mM Cs_i^+ are plotted against the membrane voltage (*V*). For comparison the dotted line, representing the best fit of the *I/V* relationship with 150 mM Na_i^+ (from Fig. 4*B* (●)) is included. A voltage-dependent block by Cs_i^+ is proposed to account for the relatively smaller inward K^+ currents at positive membrane potentials and to explain the lower *apparent* reversal potential with Cs_i^+.

a more reasonable estimate of the reversal potential but the fit to the outward Rb^+ currents was worse. For the fit giving a reversal potential of 4 mV the P_{Rb}/P_K is 0.87; the value estimated for P_K was 5.6×10^{-13} cm^3/sec (95% C.L. 5.4–5.7 × 10^{-13} cm^3/sec). From the outward Rb^+ currents the slope conductance (g_{Rb}), estimated by a linear fitting routine, was 43 pS (95% C.L. 32–53 pS).

With NH_4^+ substituted for internal K^+ and with 150 mM K_o^+ there was a good fit (r^2 = 0.99) of the *I/V* relationship (Fig. 6*A*) to the GHK equation. Values of 0.82×10^{-13} cm^3/sec (95% C.L. 0.72–0.91 × 10^{-13} cm^3/sec) and 4.8×10^{-13} cm^3/sec (95% C.L. 4.7–4.9 × 10^{-13} cm^3/sec) were obtained for P_{NH4} and P_K, respectively, and P_{NH4}/P_K was 0.17. A value of 81 pS (95% C.L. 63–99 pS) was estimated for g_{NH4} from the outward currents evoked at 60 to 90 mV.

After switching from a K^+-containing to a Cs^+-containing bath solution, the open channel current became much noisier (Fig. 6*B*) presumably due to a flickery block of the pore (Hille, 1992).

The *I/V* relationship (Fig. 6*C*) with 150 mM Cs_i^+ was comparable to that seen with 150 mM Na_i^+ in that outward currents were not seen. However, as shown in Fig. 6*C* the reversal potential of 47 mV, obtained from the best fit (unbroken line) of the data to the GHK equation, was ≈30 mV less positive than the reversal potential with 150 mM Na_i^+ (broken line of Fig. 6*C*). The fitted value for P_K and P_{Cs} in Fig. 6*C* were 4.15×10^{-13} cm^3/sec (95% C.L.

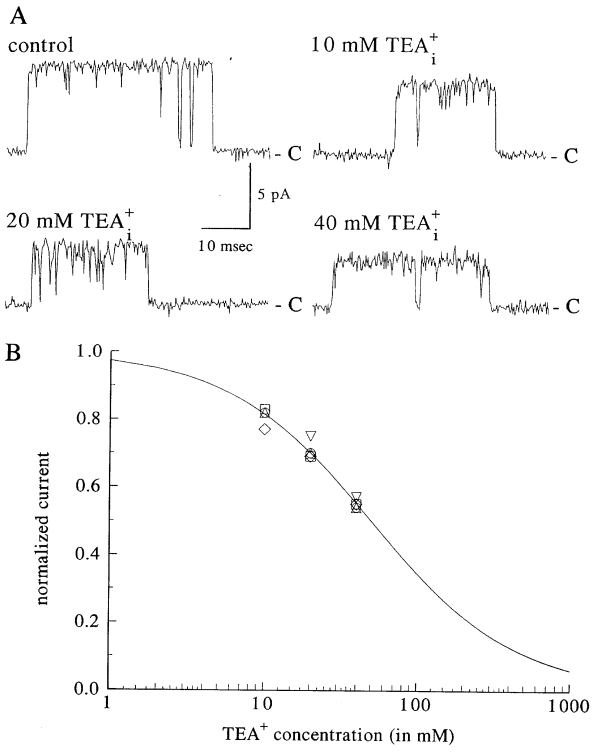

Fig. 7. (*A*) In an inside-out patch with physiological gradients for K^+ and Na^+ and at 0 mV, bath-applied (internal) TEA^+ caused a reversible, concentration-dependent reduction of the BK channel current. Note that in contrast to the situation with external TEA^+ there was little or no increase of the open channel noise. (*B*) From 4 patches, the relationship between the normalized current ($I_{TEA}/I_{control}$) and the concentration of TEA_i^+. The best fit of the data to the Hill equation gave values of 50 mM and 0.9, respectively, for the K_D(0 mV) and the Hill coefficient.

4.0–4.3 × 10^{-13} cm^3/sec) and 0.66 × 10^{-13} cm^3/sec (95% C.L. 0.15–1.17 × 10^{-13} cm^3/sec).

Pharmacology of the BK Channel

Internal TEA^+ (TEA_i^+)

In preliminary experiments, the actions of concentrations of TEA_i^+ as high as 80 mM were examined in inside-out patches with 70 mM K_i^+ and 150 mM K_o^+. Under these conditions, at −60 mV, there was no effect of TEA^+ on either the current amplitude or the P_o (*not shown*).

A blocking action of TEA^+ was observed, however, in subsequent experiments done with 10–40 mM TEA^+ in a 110 mM K^+-containing internal solution (TEA_i, Table) and with a nominally K^+-free pipette solution (150 NaCl, Table). Representative currents recorded at 0 mV in 0, 10, 20 and 40 mM TEA^+ (Fig. 7*A*) show that TEA_i^+ caused a reduction of the current amplitude but, in contrast to the situation with TEA_o^+ (*see below*), there was no obvious increase of the open channel noise. This so-called ''fast'' block arises when the mean dwell time of the blocking molecule in the channel pore is less than the response time of the recording system. Consequently, the recorded response reflects the time average of the current (Hille, 1992).

For the graph of Fig. 7*B* the normalized current ($I_{norm} = I_{TEA}/I_{control}$) has been plotted against the logarithm of the TEA^+ concentration. A fit of the data to the Hill equation,

$$I_{norm} = \frac{1}{1 + \left(\frac{[TEA^+]}{K_D}\right)^H} \tag{6}$$

gave a value of 50 mM (95% C.L. 45–55 mM) for the K_D (0 mV). The fitted value for H, the Hill coefficient, was 0.9 (95% C.L. 0.8–1.0) suggesting that a single molecule of TEA^+ is able to block the channel.

External TEA^+ (TEA_o^+)

For these experiments outside-out patches were used. The patch was held at 0 mV and there was a physiological ionic gradient (TEA_o^+ and 150 KCl solutions of the Table). As shown in Fig. 8, TEA_o^+ produced a block that was qualitatively and quantitatively different than with TEA_i^+. Much lower concentrations of TEA_o^+ caused a large reduction of the current and the block was associated with a large increase of the open channel noise, e.g., flickery block (Fig. 8*A*). From the Hill plot (Fig. 8*B*) the best-fit value for K_D (0 mV) was 0.25 mM (95% C.L. 0.21–0.29 mM). A value for H of 0.8 (95% C.L. 0.7–0.9) implied, as with TEA_i^+, that the block reflected a bimolecular reaction.

Based on analyses of 1 or 2 experiments with internal or external TEA^+ (*not shown*), the voltage-dependence of the TEA^+ block appeared to be weak. Data were fitted to the equation derived by Woodhull (1973),

$$I_{norm} = \left(1 + \frac{[TEA^+]_i}{K_D(0\text{mV})}\, e^{\frac{z\delta FV}{RT}}\right)^{-1} \quad \text{or,}$$

$$I_{norm} = \left(1 + \frac{[TEA^+]_o}{K_D(0\text{mV})}\, e^{\frac{-z\delta FV}{RT}}\right)^{-1} \tag{7}$$

in which K_D(0 mV) is the dissociation constant at 0 mV and $z\delta$ is the equivalent valence of the blocking reaction. In this case the value for $z\delta$ represents the electrical distance to the TEA^+ binding site from the side of application. With 40 mM internal TEA^+ the fitted value for $z\delta$ was .002 (95% C.L. −0.08–0.08) and K_D(0 mV) was

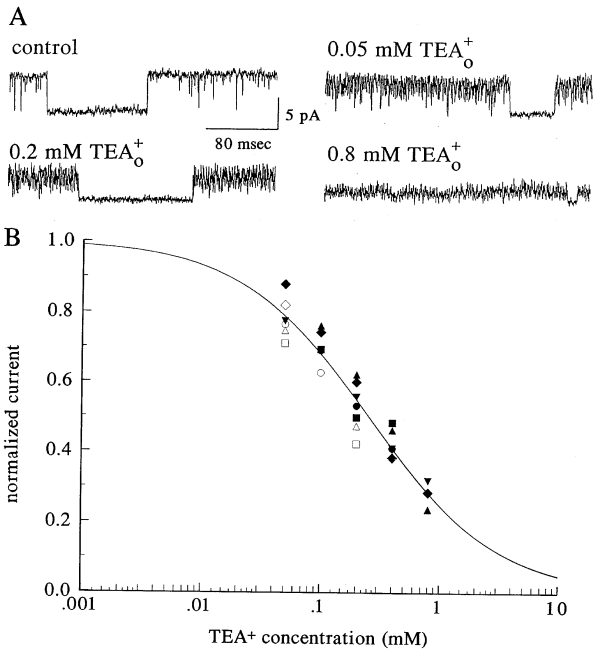

Fig. 8. The external binding site has a higher affinity for TEA^+. (*A*) These representative traces show the effect of bath-applied TEA^+ on a BK channel in an outside-out patch held at 0 mV and with physiological ionic gradients for K^+ and Na^+. TEA^+ caused a reduction of the current amplitude that was associated with increased open channel noise indicative of flickery blocking. (*B*) As for Fig. 7*B* but with TEA_o^+. Best-fit values for the K_D (0 mV) and the Hill coefficient were 0.25 mM and 0.8, respectively.

42 mM (95% C.L. 37–47 mM)(*cf.* Fig. 7*B*). In 0.4 mM TEA_o^+ the value for $z\delta$ was 0.13 (95% C.L. 0.004 to 0.24) and K_D(0 mV) was estimated to be 0.31 mM (95% C.L. 0.26–0.35 mM) which is consistent with the results of Fig. 8*B*.

Charybdotoxin

In rat muscle BK channels, where its mechanism of action has been best studied, this peptide, derived from scorpion venom, binds to a site in the external mouth of the pore with a K_D, in physiological saline, of 10 nM (Anderson et al., 1988). A long mean dwell time in the channel produces a block, described as being slow, that is detected as a concentration-dependent decrease of P_o. We investigated the actions of 40 nM charybdotoxin in outside-out patches using a pipette (internal) solution containing 150 mM KCl and a bath solution containing 140 mM NaCl (Table).

For unknown reasons it proved very difficult to obtain a stable NP_o in outside-out patches. Despite using solutions with Ca^{2+} concentrations that consistently produced a high P_o in inside-out patches, channels in the outside-out configuration, with a few exceptions, would frequently enter a closed state lasting for tens of seconds.

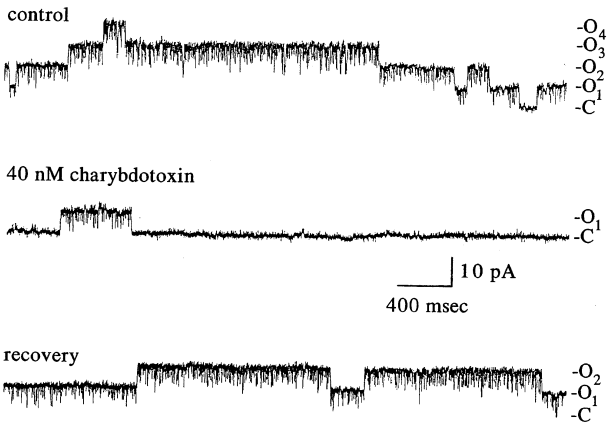

Fig. 9. Bath application of charybdotoxin to this outside-out patch held at 0 mV reduced the probability of finding BK channels in the open state but did not affect the unitary current amplitude. Near complete recovery to the control activity was obtained after returning to drug-free medium. Similar results were obtained in 3 other patches.

This behavior made a quantitative analysis impractical because, unlike the situation with TEA_o^+, the block was evident as a change of P_o rather than a decline of the amplitude of the unitary current.

We obtained 4 patches in which a fairly consistent NP_o was recorded in control and recovery responses. Representative traces are shown in Fig. 9. Charybdotoxin (40 nM) decreased NP_o to 0.01 from control and recovery values of 1.84 and 1.44, respectively. The current amplitude was unaffected by charybdotoxin.

Ca^{2+} and Voltage-dependence of BK Channel Gating

The effects of changes of the membrane voltage and $[Ca^{2+}]_i$ on the P_o of the BK channel were studied in symmetrical 150 mM K^+ (Table, 150 KCl and 0.1–10 μM Ca^{2+} solutions) in inside-out patches. With the membrane potential held at −20mV, increasing $[Ca^{2+}]_i$ from 0.1 μM to 1 μM increased the P_o from near zero to more than 0.9 (Fig. 10*A*). At a given $[Ca^{2+}]_i$, membrane depolarization could also increase P_o. This is shown in Fig. 10*B* where the voltage dependence of P_o with 0.1 μM (■), 0.5 μM (▲) and 1 μM (●) Ca^{2+} has been plotted and fitted to the Boltzmann equation,

$$P_o = \frac{P_{\max}}{1 + e^{\frac{V_{1/2} - V}{k}}} \qquad (8)$$

where $P_{\max}$ is the maximal P_o, $V_{1/2}$ is the potential at which $P_{\max}$ is half-maximal, V is the membrane potential, and k, the slope factor (mV per e-fold change), is the steepness of the voltage dependence. In the graph of Fig.

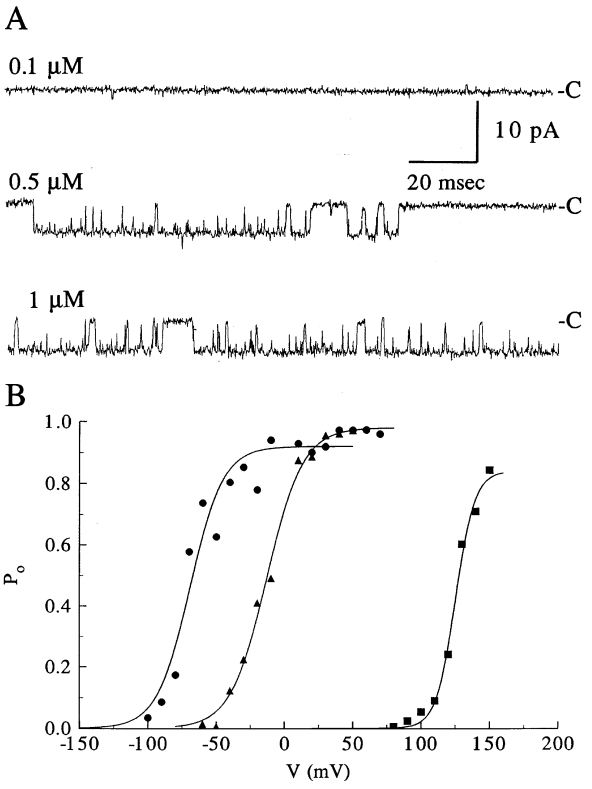

Fig. 10. BK channel gating is Ca^{2+}- and voltage-dependent. (*A*) An inside-out patch held at −20 mV in symmetrical 150 mM K^+ and containing one active BK channel shows the effect of an internal concentration of Ca^{2+} of, from above downwards, 0.1, 0.5 and 1 μM. Over this range of Ca^{2+} concentrations the P_o shifts from virtually 0 to near 1. (*B*) From the same patch as in *A*, a plot of P_o *vs. V* with Ca^{2+} concentrations of 0.1 μM (■), 0.5 μM (▲) and 1.0 μM (●). At a given concentration of Ca^{2+} the effect of membrane depolarization is to increase P_o. Values for P_{max}, $V_{½}$ and *k*, obtained from the best fit of the data to the Boltzmann equation (Eq. 8) were, respectively, 0.84, 125 mV, and 7 mV in 0.1 μM Ca^{2+}; 0.98, −13 mV and 13.4 mV in 0.5 μM Ca^{2+}; and 0.92, −69 mV and 11.9 mV in 1 μM Ca^{2+}.

10*B* the unbroken lines, drawn by using the best-fit values for $V_{1/2}$ and *k* (*see* legend of Fig. 10), are parallel but are shifted along the voltage axis by an amount that depends on the $[Ca^{2+}]_i$. In other words, *k* is unaffected by increasing $[Ca^{2+}]_i$ but $V_{1/2}$ becomes more negative.

To illustrate the variability in $V_{1/2}$ that occurred between patches the three graphs of Fig. 11 plot the P_o/V relationship in Ca^{2+} concentrations of 1 μM (*A*), 0.5 μM (*B*) and 0.1 μM (*C*). The mean (± SEM) fitted values for P_{max} and *k* in 0.1 μM Ca^{2+} (0.93 ± 0.03 and 10.1 ± 0.7 mV, respectively, $n = 6$), 0.5 μM Ca^{2+} (0.95 ± .01 and 13.6 ± 2.6 mV, $n = 5$), 1 μM Ca^{2+} (0.93 ± .01 and 9.9 ± 3.3 mV, $n = 7$) and 10 μM Ca^{2+} (0.96 ± .01 and 9.9 ± 2.6 mV, $n = 3$) were not significantly different. Of the values for $V_{1/2}$, (103.6 ± 14.8 mV, 38.7 ± 19.4 mV, −74.8 ± 8.1 mV and −62.83 ± 5.9 mV for 0.1, 0.5, 1 and 10 μM, respectively) only those for 1 and 10 μM Ca^{2+} were not significantly different.

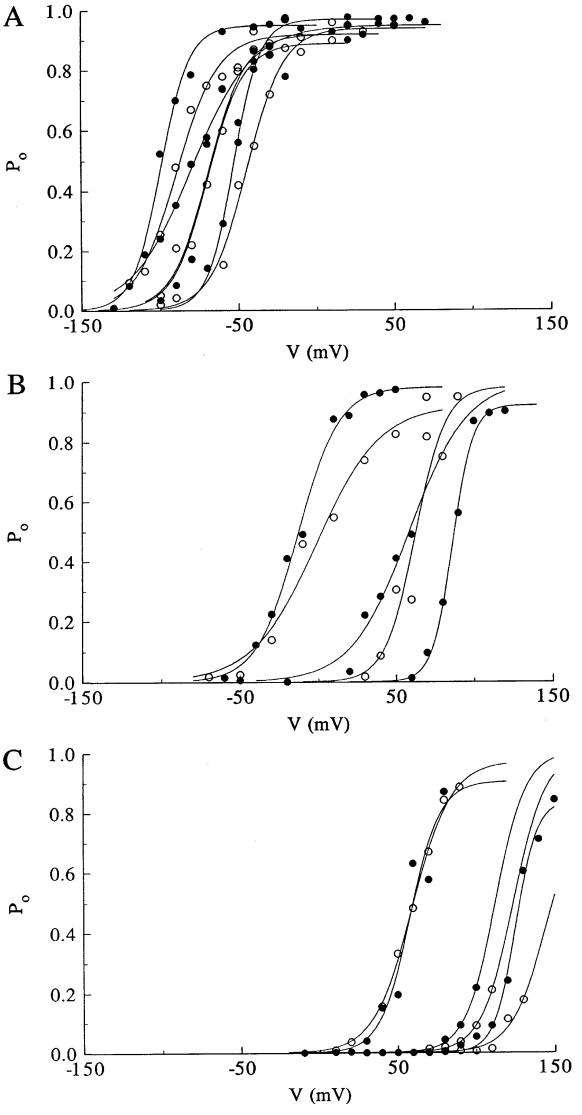

Fig. 11. The P_o/V relationship in Ca^{2+} concentrations of, from above downwards, 1 μM (7 patches), 0.5 μM (5 patches) and 0.1 μM (6 patches). Open and filled circles have been used to help distinguish different curves but have no other significance within or between the graphs.

To estimate the number of Ca^{2+} binding sites on the BK channel, we used an equation derived by Wong, Lecar & Adler (1982),

$$\frac{V_{1/2}}{k} = N_{Ca} \ln\left(\frac{K_D(0mV)}{[Ca^{2+}]_i}\right) \quad (9)$$

that is based on the assumption that Ca^{2+} binding is highly cooperative and voltage-dependent. In the equation, N_{Ca} is the number of Ca^{2+} binding sites and is analogous to the Hill coefficient; the other variables have been defined previously. Values for $V_{1/2}$ and *k* were

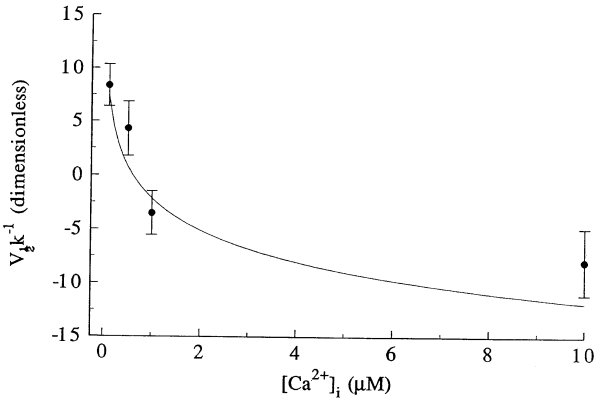

Fig. 12. The best-fit line describing the relationship (Eq. 9) between the half-activation potential ($V_{1/2}$) divided by the slope factor (k) and the Ca^{2+} concentration gives an estimate of 4 (range 3–6) for the number of Ca^{2+} binding sites on the melanotroph BK channel.

taken from Fig. 11 and other data not shown. For the best-fit line of Fig. 12 ($r^2 = 0.64$) N_{Ca} was 4.2 (95% C.L. 2.6–5.8) and K_D(0 mV) was 0.47 μM (95% C.L. 0.17–0.78 μM).

Discussion

Melanotroph BK channels have a conductance in 150 mM symmetrical K^+ of approximately 260 pS. Similar conductances have been reported for BK channels of bovine chromaffin cells (265 pS in 160 mM K^+) (Yellen, 1984*a*), clonal GH_3 pituitary cells (250–300 pS in 150 mM K^+) (Lang & Ritchie, 1987) and rabbit T-tubules (260 pS in 100 mM K^+) (Vergara, Moczydlowski & Latorre, 1984). Clonal AtT-20 pituitary cells have a slightly smaller conductance (208 pS in 145 mM K^+) (Wong, Lecar & Adler, 1982).

It is difficult to estimate the BK channel conductance under physiological conditions given the uncertainty concerning $a_{K,i}$. We estimated values of 86 mM and 113 mM for $a_{K,i}$ and $[K^+]_i$, respectively, from cell-attached recordings. By comparison, a value of 83 mM has been reported for $a_{K,i}$ in heart muscle (Lee & Fozzard, 1975) and values of 107, 122 and 114 mM have been reported, respectively, for $[K^+]_i$ in cultured cortical (White et al., 1992) and hippocampal (Bulan, Barker & Mienville, 1994) neurones and pancreatic β cells (Smith, Ashcroft & Fewtrell, 1993). Assuming an $a_{K,i}$ of 86 mM, an $a_{K,o}$ of 3.5 mM and an absolute K^+ permeability of 6×10^{-13} cm^3/sec the slope conductance at 0 mV would be approximately 140 pS.

The permeability (selectivity) sequence, K^+ (1) > Rb^+ (0.87) > NH_4^+ (0.17) > $Cs^+ \geqslant Na^+$ (<0.02), is virtually the same as that for the BK channel of chromaffin cells ($K^+ > Rb^+$ (0.83) > Cs^+, Na^+ (<.03) (Yellen, 1984*a*) and similar to that in rabbit T-tubules (K^+ (1) > Rb^+ (0.7) > NH_4^+ (0.15) > Cs^+,Na^+) (Vergara et al., 1984). Our estimates of g_{Rb} and g_{NH4} slope conductances of 40 pS and 83 pS, respectively, are comparable to those reported in smooth muscle (≈30 pS in symmetrical 126 mM Rb^+) (Benham et al., 1986) or T-tubules (22 pS and 56 pS, respectively, in 300 mM Rb^+ and NH_4^+) (Eisenman, Latorre & Miller, 1986). These estimates give a conductance sequence ($g_K > g_{NH4} > g_{Rb}$) in which Rb^+ and NH_4^+ are transposed vis-à-vis the permeability sequence, as is also the case with T-tubule BK channels (Eisenman et al., 1986). As discussed by Hille (1992) the relative permeability is governed primarily by the highest energy peak or barrier to ion passage whereas the conductance reflects additional contributions of energy wells or binding sites within the channel pore. Consequently, a Rb^+ conductance lower than that for K^+ or NH_4^+ might reflect a longer mean dwell time of Rb^+ at a binding site in the channel pore.

The low Na^+ permeability of the BK channel is important from a functional standpoint since, in physiological ionic gradients, the open BK channel effectively passes only outward, hyperpolarizing currents carried by K^+. That Na^+ is unable to permeate the channel has been attributed to its small diameter (0.19 nm). Hille (1992) suggests its small size prevents an interaction of Na^+ with a ring of carboxyl oxygens in the pore wall. Such an interaction is necessary to make it energetically favorable for the hydrated ion to lose some water molecules from its hydration ''shell,'' reduce its size and continue on past this site.

In BK channels of chromaffin cells (Yellen, 1984*b*) and T-tubules (Latorre, 1986), internal Na^+ causes a strongly voltage-dependent channel block and the same effect is seen with melanotroph BK channels (S.J. Kehl, *unpublished observation*). That no such blocking action was evident in the bi-ionic recording conditions with 150 mM Na_i^+ might have been due to the relieving effect of the high external concentration of K^+ (Yellen, 1984*b*).

Although we cannot exclude an allosteric mechanism of action, the flickering of inward K^+ currents with 150 mM Cs_i^+ is compatible with the view that Cs^+ is able to enter and block the internal mouth of the BK pore. Flickery block with high concentrations of Cs_i^+ has also been seen with smooth muscle BK channels (Benham et al., 1986). Interestingly, the block by Cs_i^+ of chromaffin BK channels is different in that, first, much lower concentrations (10 mM) of Cs_i^+ are effective, and, second, the block is fast (Yellen, 1984*a*). This is the only property we found that clearly discriminated melanotroph and chromaffin cell BK channels.

Outward Cs^+ currents were never detected but the extrapolated reversal potential with 150 mM Cs_i^+ was approximately 30 mV less than it was with 150 mM Na_i^+. A similar finding has been reported both for smooth muscle BK channels, where the reversal potential with

Cs_i^+ was between 40 and 50 mV (Benham et al., 1986), and for chromaffin cell BK channels (Yellen, 1984*a*), where the reversal potential was near −50 mV with 160 mM Cs_o^+ and 160 mM K_i^+. This might mean that P_{Cs} is greater than P_{Na} however there is an another possible explanation. If, as in other BK channels (Yellen, 1984*a*; Cecchi et al., 1987), the Cs^+ blocking site is in the pore itself and within the electrical field, then depolarization would be expected to increase the affinity of the block by Cs_i^+. Consequently, and to an extent depending on the values for $z\delta$ and K_D(0 mV), the *I/V* plot would approach the voltage axis in a manner that could cause an underestimation of the reversal potential. Our data are therefore consistent with the suggestions of others (Latorre & Miller, 1983; Benham et al., 1986) that Cs^+ can enter but, because of its size (0.338 nm *vs.* 0.266 nm for K^+), cannot pass completely through the BK channel pore for which a minimum diameter of 0.3 nm has been proposed (Latorre & Miller, 1983). This minimum diameter can account for the permeability of Rb^+ which has a diameter of 0.296 nm, and, although it is larger than the 0.3 nm limitation, the permeability of the NH_4^+ ion (0.304 nm diameter) might reflect its ability to hydrogen bond with carboxyl groups of the pore wall (Latorre & Miller, 1983).

Our results with TEA^+ follow the established pattern that external TEA^+ is a more potent inhibitor of BK channels than is internal TEA^+. The K_Ds of 0.25 and 50 mM, respectively, for the block by external and internal TEA^+ are also similar to those reported for the BK channel of skeletal smooth muscle cells ($K_{D,TEAo}$ = 0.3 mM; $K_{D,TEAi}$ = 35 mM) (Vergara et al., 1984) and bovine adrenal chromaffin cells ($K_{D,TEAo}$ = 0.2 mM; $K_{D,TEAi}$ = 27 mM) (Yellen, 1984*a*). The internal TEA binding site on the BK channel of clonal GH_3 anterior pituitary cells has a K_D of 0.26 mM (Lang & Ritchie, 1990). At least with regard to the TEA^+ binding sites, BK channels of pituitary melanotrophs are clearly structurally distinct from BK channels of clonal AtT-20 anterior pituitary cells (Wong & Adler, 1986) where the opposite profile of TEA^+ sensitivity is observed ($K_{D,TEAi}$ = 0.08 mM; $K_{D,TEAo}$ = 52 mM).

Interestingly, we found no significant blocking effect with 80 mM TEA_i^+ when the external solution contained 150 mM K_o^+. In their studies of smooth muscle BK channels Benham et al. (1985) also noted that concentrations of TEA_i^+ up to 50 mM were ineffective in symmetrical 126 mM K^+ whereas with a physiological K^+ gradient (126 mM K_i and 6 mM K_o) half-maximal block occurred with approximately 12 mM TEA_i^+. One interpretation of these data is that TEA^+ and K_o^+ compete for a binding site within the pore (*see also* Taglialatela et al., 1993).

The weak voltage dependence of TEA^+ binding to either the internal or external site reported here and elsewhere (Yellen, 1984*a*; Lang & Ritchie, 1990), together with values for the Hill coefficient consistently near 1, indicate that a single TEA^+ molecule moving only a small distance into the electrical field is able to block the BK channel. A simple structural interpretation of these data is that TEA^+, which has the same radius as hydrated K^+ (0.8 nm) (Latorre & Miller, 1983), enters only part way into the channel before further electrodiffusion is prevented by a narrowing of the pore.

In agreement with the preliminary report of Wang & Lemos (1992) charybdotoxin blocked the melanotroph BK channel and thus fits into the Type I category (Tseng-Crank et al., 1994). We have not yet studied the effect of charybdotoxin on the voltage-gated K^+ channels of melanotrophs and cannot comment on its specificity.

The gating of melanotroph BK channels is both voltage- and Ca^{2+}-dependent. The value for *k*, which represents the steepness of the voltage dependence, was unaffected by $[Ca^{2+}]_i$ and is similar (10–13 mV per *e*-fold change) to that reported for most other BK channels (Latorre et al., 1989). And, as with most BK channels, increases of $[Ca^{2+}]_i$ can increase P_o to a value near 1 (*see* Sugihara, 1994 for an exception). Melanotroph BK channels have a Ca^{2+} sensitivity that is similar to that of clonal AtT-20 pituitary cells (Wong, Lecar, & Adler, 1982), greater than that of T-tubules (Anderson et al., 1988) or hair cells (Art, Wu & Fettiplace, 1995) and less than that of pancreatic acinar cells (Maruyama et al., 1983). There was however considerable variability of the P_o between channels, as has been reported for rat muscle BK channels (Moczydlowski & Latorre, 1983) where ''[the P_o of] different channels can vary by as much as 0.8 P_o units at the same voltage and Ca^{2+} concentration.'' The best fit of the relationship between P_o and the $[Ca^{2+}]_i$ gave an estimate of 4 for the number (N_{Ca}) of Ca^{2+} binding sites on melanotroph BK channels. In other types of tissue, the estimates for N_{Ca} vary. For example, in skeletal muscle values of 2 (Moczydlowski & Latorre, 1983), 3 (Barrett et al., 1982) and 6 (Golowasch, Kirkwood & Miller, 1986) have been reported for N_{Ca}. In clonal pituitary cells $N_{Ca}\approx 3$ (Wong, Lecar & Adler, 1982). An hypothesis that we have not yet tested is that the variability of the Ca^{2+} sensitivity reflects the phosphorylation state of the channel (White, Schonbrunn & Armstrong, 1991) or the existence of dissociable subunits.

We thank Michael D. Mitton and Kamran Kheirani for their assistance with some of the experiments. Supported by a grant to S.J.K. from the Natural Sciences and Engineering Resource Council (NSERC) of Canada.

References

Anderson, C.S., MacKinnon, R., Smith, C., Miller, C. 1988. Charybdotoxin block of single Ca^{2+}-activated K^+ channels. *J. Gen. Physiol.* **91:**317–333

Art, J.J., Wu, Y.-C., Fettiplace, R. 1995. The calcium-activated potassium channels of turtle hair cells. *J. Gen. Physiol.* **105:**49–72

Barrett, J.N., Magleby, K.L., Pallotta, B.S. 1982. Properties of single calcium-activated potassium channels in cultured rat muscle. *J. Physiol.* **331:**211–230

Benham, C.D., Bolton, T.B., Lang, R.J., Takewaki, T. 1985. The mechanism of action of Ba^{2+} and TEA on single Ca^{2+}-activated K^+-channels in arterial and intestinal smooth muscle membranes. *Pfluegers Arch.* **403:**120–127

Benham, C.D., Bolton, T.B., Lang, R.J., Takewaki, T. 1986. Calcium-activated potassium channels in single smooth muscle cells of rabbit jejunum and guinea-pig mesenteric artery. *J. Physiol.* **371:**45–67

Blatz, A.L., Magleby, K.L. 1984. Ion conductance and selectivity of single calcium-activated potassium channels in cultured rat muscle. *J. Gen. Physiol.* **84:**1–23

Blatz, A.L., Magleby, K.L. 1986. Single apamin-blocked Ca-activated K^+ channels of small conductance in cultured rat skeletal muscle. *Nature* **323:**718–720

Bulan, E.J., Barker, J.L., Mienville, J.-M. 1994. Immature maxi-K channels exhibit heterogeneous properties in the embryonic rat telencephalon. *Dev. Neurosci.* **16:**25–33

Cecchi, X., Wolff, D., Alvarez, O., Latorre, R. 1987. Mechanisms of Cs^+ blockade in a Ca^{2+}-activated K^+ channel from smooth muscle. *Biophys. J.* **52:**707–716

Cota, G. 1986. Calcium channel current in pars intermedia cells of the rat pituitary gland. *J. Gen. Physiol.* **88:**83–105

Eisenman, G., Latorre, R., Miller, C. 1986. Multi-ion conduction and selectivity in the high conductance Ca^{++}-activated K^+ channel from skeletal muscle. *Biophys. J.* **50:**1025–1034

Golowasch, J., Kirkwood, A., Miller, C. 1986. Allosteric effects of Mg^{2+} on the gating of Ca^{2+}-activated K^+ channels from mammalian skeletal muscle. *J. Exp. Biol.* **124:**5–13

Hille, B. 1992. Ionic channels of excitable membranes. Sinauer, Sunderland

Kehl, S.J., Hughes, D., McBurney, R.N. 1987. A patch clamp study of γ-aminobutyric acid (GABA)-induced macroscopic currents in rat melanotrophs in cell culture. *Br. J. Pharmacol.* **92:**573–585

Kehl, S.J., Kheirani, K., Mitton, M., Wong, K. 1995. Properties of Ca^{2+}-dependent, large conductance K (BK) channels in cultured rat melanotrophs. *Soc. Neurosci. Abstr.* **21:**1825

Lang, D.G., Ritchie, A.K. 1987. Large and small conductance calcium-activated potassium channels in the GH_3 anterior pituitary cell line. *Pfluegers Arch.* **410:**614–622

Lang, D.G., Ritchie, A.K. 1990. Tetraethylammonium blockade of apamin-sensitive and insensitive Ca^{2+}-activated K^+ channels in a pituitary cell line. *J. Physiol.* **425:**117–132

Latorre, R. 1986. The large calcium-activated potassium channel. *In:* Ion Channel Reconstitution. C. Miller, editor. pp. 431–467. Plenum Press, New York

Latorre, R., Miller, C. 1983. Conduction and selectivity in potassium channels. *J. Membrane Biol.* **71:**11–30

Latorre, R., Oberhauser, A., Labarca, P., Alvarez, O. 1989. Varieties of calcium-activated potassium channels. *Ann. Rev. Physiol.* **51:**385–399

Lee, C.O., Fozzard, H.A. 1975. Activities of potassium and sodium ions in rabbit heart muscle. *J. Gen. Physiol.* **65:**695–708

Martell, A.E., Smith, R.M. 1974. Critical Stability Constants. Vol 1. Plenum, London

Maruyama, Y., Petersen, O.H., Flanagan, P., Pearson, G.T. 1983. Quantification of Ca^{2+}-activated K^+ channels under hormonal control in pig pancreas acinar cells. *Nature* **305:**228–232

McBurney, R.N., Kehl, S.J. 1988. Electrophysiology of neurosecretory cells from the pituitary intermediate lobe. *J. Exp. Biol.* **139:**317–328

Moczydlowski, E., Latorre, R. 1983. Gating kinetics of Ca^{2+}-activated K^+ channels from rat muscle incorporated into planar bilayers. *J. Gen. Physiol.* **82:**511–542

Muraki, K., Imaizumi, Y., Watanabe, M. 1992. Ca-dependent K channels in smooth muscle cells permeabilized by β-escin recorded using the cell-attached patch-clamp technique. *Pfluegers Arch.* **420:**461–469

Robinson, R.A., Stokes, R.H. 1965. Electrolyte Solutions. Butterworths, London

Smith, P.A., Ashcroft, F.M., Fewtrell, C.M.S. 1993. Permeation and gating properties of the L-type calcium channel in mouse pancreatic β cells. *J. Gen. Physiol.* **101:**767–797

Sugihara, I. 1994. Calcium-activated potassium channels in goldfish hair cells. *J. Physiol.* **476:**373–390

Taglialatela, M., Drewe, J.A., Kirsch, G.E., De Biasi, M., Hartmann, H.A., Brown, A.M. 1993. Regulation of K^+/Rb^+ selectivity and internal TEA blockade by mutations at a single site in K^+ pores. *Pfluegers Arch.* **423:**104–112

Tseng-Crank, J., Foster, C.D., Krause, J.D., Mertz, R., Godinot, N., DiChiara, T.J., Reinhart, P.H. 1994. Cloning, expression, and distribution of functionally distinct Ca^{2+}-activated K^+ channel isoforms from human brain. *Neuron* **13:**1315–1330

Vergara, C., Moczydlowski, E., Latorre, R. 1984. Conduction, blockade and gating in a Ca^{2+}-activated K^+ channel incorporated into planar lipid bilayers. *Biophys. J.* **45:**73–76

Wang, G., Lemos, J.R. 1992. Regulation of Ca^{2+}-activated K^+ channel in nerve terminals of the rat neurohypophysis. *Soc. Neurosci. Abstr.* **18:**72

White, H.S., Chow, S.Y., Yen-Chow, Y.C., Woodbury, D.M. 1992. Effect of elevated potassium on the ion content of mouse astrocytes and neurons. *Can. J. Physiol. Pharmacol.* **70:**S263–S268

White, R.E., Schonbrunn, A., Armstrong, D.L. 1991. Somatostatin stimulates Ca^{2+}-activated K^+ channels through protein dephosphorylation. *Nature* **351:**570–573

Wong, B.S., Adler, M. 1986. Tetraethylammonium blockade of calcium-activated potassium channels in clonal anterior pituitary cells. *Pfluegers Arch.* **407:**279–284

Wong, B.S., Lecar, H., Adler, M. 1982. Single calcium-dependent potassium channels in clonal anterior pituitary cells. *Biophys. J.* **39:**313–317

Woodhull, A.M. 1973. Ionic blockage of sodium channels in nerve. *J. Gen. Physiol.* **61:**687–708

Yellen, G. 1984*a*. Ionic permeation and blockade in Ca^{2+}-activated K^+ channels of bovine chromaffin cells. *J. Gen. Physiol.* **84:**157–186

Yellen, Y. 1984*b*. Relief of Na^+ block of Ca^{2+}-activated K^+ channels by external cations. *J. Gen. Physiol.* **84:**187–199